Memoirs of the Faculty of Engineering and Design
Kyoto Institute of Technology 53 (March, 2005)

Micromechanical Analysis of Macroscopic Stiffness of a SMP Intelligent Composite Material

Hiroyuki ONO

(Received September 17, 2004; Accepted December 13, 2004)

Abstract

A shape memory polymer (SMP) whose glass transition temperature T_g can be designed has both the shape memory effect and the shape fixity effect. In our previous research, by analyzing an intelligent composite material containing the SMP particles, the macroscopic stiffness of the material can change according to the type of the distribution of T_g and the magnitude of the shape memory shrinkage of the SMP particle. In the analysis, the shape of the SMP particle is assumed to be a spherical shape. However, when the shape of the SMP reinforcement is a spheroid or a cylinder, the macroscopic stiffness of the composite in the longitudinal direction of the reinforcement differs from that in its lateral direction. Namely, the property of the material on the stiffness shows anisotropy. This property can change due to the shape of the SMP reinforcement. The shape of the SMP reinforcement does not change by the constraint from the matrix surrounding the reinforcement, as the reinforcement change from the rubber state to the glass one. In this study, by taking into consideration such a shape fixity effect of the SMP reinforcement, micromechanical modeling and analysis are performed for an intelligent composite material containing SMP reinforcements and the change in degree of anisotropy of the material on the stiffness is examined. The macroscopic elastic modulus of the material is formulated as a function of the aspect ratio of the reinforcement. By using the expression obtained above, we can change the value of the macroscopic elastic modulus by changing the aspect ratio of the reinforcement. Especially, for the spheroidal reinforcement, we find that there are two aspect ratios that values of the macroscopic elastic modulus in the longitudinal direction of the reinforcement are same each other, and values of the macroscopic elastic modulus in the lateral direction of the reinforcement obtained from these aspect ratios are different from each other. As the result, we can suggest that it is possible to change degree of anisotropy of the material on the stiffness by utilizing the shape fixity effect of the SMP reinforcement.

Key Words: *Micromechanics ; Intelligent material ; Shape memory polymer ; Shape fixity effect ; Macroscopic elastic modulus ; Anisotropy*

1. Introduction

Recently, for intelligent composite materials containing a piezoelectric reinforcement or a shape memory one, it has been examined experimentally to give following functions to the materials, i.e., (1) sensor function and (2) actuator one. For example, for a composite

material containing the piezoelectric reinforcement, it is possible to detect a deformation or a damage in the material by the electric current occurred in a piezoelectric reinforcement[1]. Such a sensor function is known as health-monitoring. For a composite material containing TiNi shape memory alloy fibers, a crack surface in the material can be closed by the shape memory shrinkage of the fiber[2]. By such an actuator function, the toughness of the material is improved.

In our previous research[3–6], for the composite material containing TiNi shape memory fibers or shape memory polymer(SMP) particles, it is possible to change the magnitude of the macroscopic stiffness of the composite by using properties of these shape memory reinforcements. A shape memory polymer whose glass transition temperature T_g can be designed has both the shape memory effect and the shape fixity effect. For example, the composite material containing SMP particles, we showed analytically that it was possible to change the path of the macroscopic stiffness of the material with the temperature by changing the type of the distribution of the glass transition temperature of the SMP particle[4]. Moreover, we indicated that the magnitude of the macroscopic stiffness of the material could change in according to the magnitude of the shape memory shrinkage of the SMP particle[5, 6]. From these results, the change in the stiffness of the material is divided into two following categories:

(1) The path of the macroscopic stiffness of the composite material with temperature.

(2) The change in the magnitude of the macroscopic stiffness of the composite material to a desirable one.

In these studies, the shape of the SMP particle is assumed to be a sphere. However, when the shape of the SMP particle is a oblate spheroid or a cylinder, the macroscopic stiffness of the composite material in the longitudinal direction of the SMP reinforcement differs from that in its lateral direction. Namely, the property of the material on the stiffness becomes to be anisotropy. Therefore, in addition to two categories mentioned above, another change in the stiffness of the material can be thought as follows.

(3) The change in the ratio of the macroscopic stiffness in one direction to that in other direction, that is, degree of anisotropy of the material on the stiffness.

The key to change degree of anisotropy of the material is the shape of the SMP reinforcement.

A SMP material has not only the shape memory effect but also the shape *fixity effect*[7]. For the composite material containing the SMP reinforcement, the shape of the SMP reinforcement does not change due to the constraint from the matrix surrounding the SMP reinforcement, as the SMP reinforcement changes from the rubber state to the glass one during the cooling process of the material. Moreover, when the SMP reinforcement becomes to be the glass state, residual stresses do not occur in the material. By using such a shape *fixity* effect of the SMP reinforcement, we may change degree of anisotropy of the material on the stiffness.

In this study, micromechanical analysis of an intelligent composite material containing the SMP reinforcement will be performed by taking into consideration the shape fixity effect of the SMP reinforcement. The shape of the SMP reinforcement is modeled as *an ellipsoid* and the macroscopic elastic modulus of the material will be formulated in terms of the aspect ratio of the SMP reinforcement. By using the expression obtained above, we will

numerically calculate the effect of the aspect ratio of the SMP reinforcement on the macroscopic elastic modulus of the material. From this result, we examine the ratio of the macroscopic elastic modulus in the longitudinal direction of the SMP reinforcement to that in its lateral direction, that is, degree of anisotropy of the material on the stiffness, by utilizing the shape fixity effect of the SMP reinforcement.

2. Analysis of macroscopic elastic moduli of a SMP intelligent composite material

2.1 Shape fixity effect of a SMP material

The shape fixity effect[7] of a SMP material is explained schematically in Figure 1. The SMP material in the rubber state at the temperature T over its glass transition temperature T_g is shown in Fig. 1(a). When an external force P is applied to the SMP material, the SMP material is elongated as shown in Fig. 1(b). The external force is kept in constant and the SMP material is cooled to the temperature lower than its T_g. Then, the SMP material translates to the glass state. This is shown in Fig. 1(c). When the external force is removed, the SMP material cannot shrink to the original shape and can keep in the deformed shape as shown in Fig. 1(d). This effect is called as the shape fixity one.

2.2 Analytical model

We consider a composite material containing many SMP reinforcements. We assume that all of SMP reinforcements have a same glass transition temperature T_g, and they are embedded in a matrix when they are in the rubber state at the temperature over T_g. When the material is cooled to the temperature lower than T_g, the shape of the SMP reinforcement in the rubber state is fixed by the constraint from the matrix surrounding the SMP reinforcement. During this cooling process, the thermal expansion strain will be occurred in the SMP reinforcement due to the mismatch between the thermal expansion coefficients of the SMP reinforcement and the matrix. The SMP reinforcement cannot expand freely by the thermal expansion strain because the SMP reinforcement is constrained by the surrounding matrix. Therefore, the thermal stress occurs in the material. However, the thermal expansion strain in the SMP reinforcement vanishes completely after the shape of the SMP reinforcement is fixed, therefore, the effect of the thermal expansion strain is ignored at any temperature.

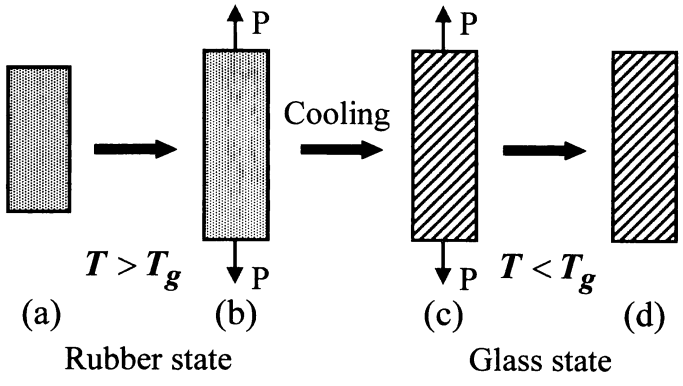

Fig. 1 Shape fixity effect of the SMP material.

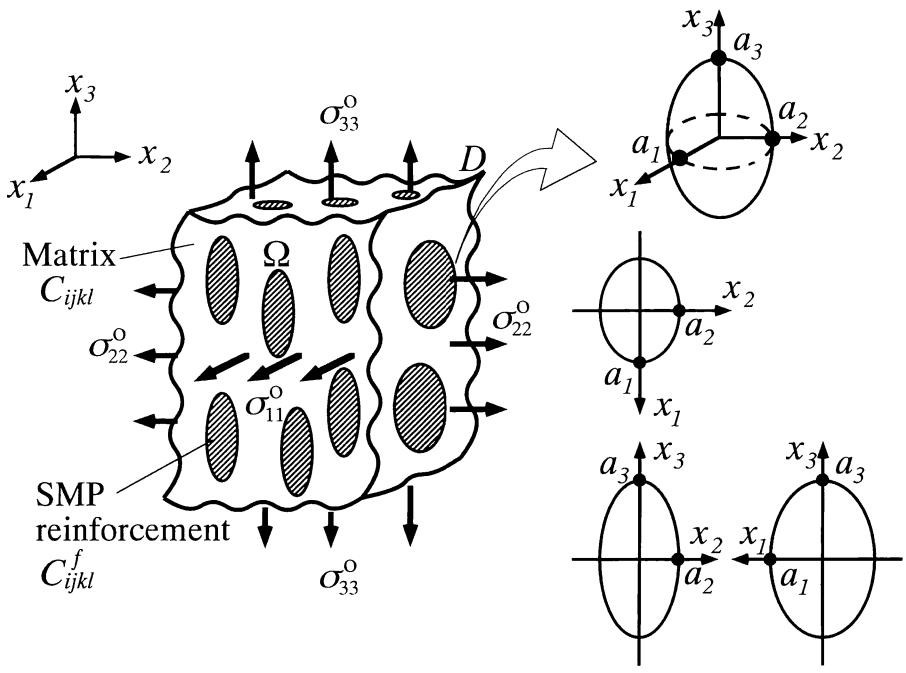

Fig. 2 Intelligent composite material containing SMP reinforcements.

The analytical model of the composite material containing the SMP reinforcement is shown in Figure 2. The region occupied by the SMP reinforcement is indicated by the shaded part in Fig. 2. This region is denoted by Ω, and the region of the whole body of the material is denoted by D. The shape of the SMP reinforcement is assumed to be an ellipsoid. The SMP reinforcements of the same geometry and the same orientation are assumed to be arranged randomly in the matrix. Dimensions of this ellipsoid in the directions of the principal half axes are a_1, $a_2 = a_1\omega_2$, $a_3 = a_1\omega_3$, where ω_2 and ω_3 are aspect ratios of the SMP reinforcement, respectively. This shape is shown in the right hand of Fig. 2. To fix the shape of the SMP reinforcement, the material will be cooled from the temperature higher than T_g to that lower than T_g. In this cooling process, the SMP reinforcement becomes to be the rubber state, the transition one, and the glass one in turn. This change of the state will be considered when analyzing the model. Moreover, the external stresses σ^0_{11}, σ^0_{22}, and σ^0_{33} apply to the composite material.

2.3 Equivalent equation for a SMP reinforcement

The region Ω of the SMP reinforcement can be treated as an inhomogeneity whose elastic constants are different from those of the matrix. Thus, the equivalent equation to replace such a region Ω with an homogeneous inclusion whose elastic constants are same of those of the matrix is expressed as follows:

$$\sigma^0_{ij} + \tilde{\sigma}_{ij} + \sigma^\infty_{ij} = C^f_{ijkl}(\varepsilon^0_{kl} + \tilde{\varepsilon}_{kl} + S_{klmn}\varepsilon^*_{mn}) = C_{ijkl}(\varepsilon^0_{kl} + \tilde{\varepsilon}_{kl} + S_{klmn}\varepsilon^*_{mn} - \varepsilon^*_{kl}), \tag{1}$$

where ε^*_{ij} is an equivalent eigenstrain which is given to the region Ω, and C^f_{ijkl} and C_{ijkl} are the elastic constants of the SMP reinforcement and the matrix, respectively. σ^∞_{ij} is the

eigenstress of the SMP reinforcement and S_{ijkl} is the Eshelby tensor[8] for the SMP reinforcement. Araki et al. indicate that Eshelby tensor can be expressed by two factors, the one is concerned with the aspect ratio of SMP reinforcement and the other with the Poisson's ratio ν of the matrix[9]. For example, S_{1111} and S_{1122} are expressed as,

$$S_{1111}=H_1^e+\frac{1}{2(1-\nu)}\left\{(H_1^e-H_{12}^e)+(H_3^e-H_{31}^e)\right\}, \tag{2-a}$$

$$S_{1122}=\frac{\nu}{1-\nu}H_1^e-\frac{1}{2(1-\nu)}(H_1^e-H_{12}^e), \tag{2-b}$$

where H_i^e and H_{ij}^e are expressed in terms of only aspect ratios ω_2 and ω_3 of the SMP reinforcement as follows[9]:

$$H_2^e=\frac{1}{\omega_2^2-1}\left\{\frac{\omega_2\omega_3F(\theta,k)}{(\omega_2^2-\omega_3^2)^{1/2}}-\frac{\omega_2\omega_3E(\theta,k)}{(\omega_2^2-\omega_3^2)^{1/2}}\right\}, \tag{3-a}$$

$$H_3^e=\frac{1}{1-\omega_3^2}\left\{1-\frac{\omega_2\omega_3E(\theta,k)}{(\omega_2^2-\omega_3^2)^{1/2}}\right\}, \tag{3-b}$$

$$H_1^e+H_2^e+H_3^e=1, \tag{3-c}$$

$$H_{12}^e=\frac{\omega_3^2}{1-\omega_2^3}(H_2^e-H_1^e), \tag{3-d}$$

$$H_{23}^e=\frac{\omega_2^2}{\omega_3^2-\omega_2^3}(H_3^e-H_2^e), \tag{3-e}$$

$$H_{31}^e=\frac{1}{\omega_2^2-1}(H_1^e-H_3^e), \tag{3-f}$$

$$H_{21}^e=\frac{1}{1-\omega_3^2}(H_2^e-H_1^e), \tag{3-g}$$

$$H_{32}^e=\frac{\omega_3^2}{\omega_3^2-\omega_2^2}(H_3^e-H_2^e), \tag{3-h}$$

$$H_{13}^e=\frac{\omega_2^2}{\omega_2^2-1}(H_1^e-H_3^e). \tag{3-i}$$

In eq.(3), $F(\theta,k)$ and $E(\theta,k)$ are the incomplete elliptic integrals of the first and the second kind, respectively, and θ and k are given by

$$\theta=sin^{-1}\left(1-\frac{\omega_3^2}{\omega_2^2}\right)^{1/2}, \qquad k=\left(\frac{\omega_2^2-1}{\omega_2^2-\omega_3^2}\right)^{1/2}. \tag{4}$$

Araki et al. name H_i^e and H_{ij}^e the geometrical factor[9]. Other components of S_{ijkl} in eq.(2) can be obtained by the cyclic permutation of (1,2,3).

For the spheroidal SMP reinforcement with $a_1=a_2$, the relationships between H_i^e and H_{ij}^e are given by[9]

$$H_1^e = H_2^e = \frac{1}{2}(1 - H_3^e), \tag{5-a}$$

$$H_{12}^e = \frac{1}{4}(1 - H_{31}^e), \tag{5-b}$$

$$H_{13}^e = H_{23}^e = \frac{1}{2} - \frac{3}{2}H_3^e + H_{31}^e. \tag{5-c}$$

In this case, there are two independent geometrical factors, H_3^e and H_{31}^e. The values of H_3^e and H_{31}^e for various types of spheroid are written as follows[9]:

1) Oblate spheroid ($a_1 = a_2 > a_3$)

$$H_3^e = 1 - \frac{\omega_3}{(1-\omega_3^2)^{3/2}}\left\{\cos^{-1}\omega_3 - \omega_3(1-\omega_3^2)^{1/2}\right\}, \tag{6-a}$$

$$H_{31}^e = -\frac{1-3H_3^e}{2(1-\omega_3^2)}, \quad (0 < \omega_3 < 1). \tag{6-b}$$

2) Sphere ($a_1 = a_2 = a_3$)

$$H_3^e = \frac{1}{3}, \quad H_{31}^e = \frac{1}{5}, \quad (\omega_3 = 1). \tag{7}$$

3) Prolate spheroid ($a_1 = a_2 < a_3$)

$$H_3^e = 1 - \frac{\omega_3}{(\omega_3^2-1)^{3/2}}\left\{\omega_3(\omega_3^2-1)^{1/2} - \cosh^{-1}\omega_3\right\}, \tag{8-a}$$

$$H_{31}^e = -\frac{1-3H_3^e}{2(\omega_3^2-1)}, \quad (\omega_3 > 1). \tag{8-b}$$

4) Cylinder ($a_1 = a_2$, $a_3 \to \infty$)

$$H_3^e = H_{31}^e = 0, \quad (\omega_3 \to \infty). \tag{9}$$

For the elliptic cylindrical reinforcement with $a_3 \to \infty$, the value of H_i^e and H_{ij}^e are given by

$$H_1^e = \frac{\omega_2}{1+\omega_2}, \quad H_2^e = \frac{1}{1+\omega_2}, \quad H_3^e = 0, \tag{10-a}$$

$$H_{12}^e = \frac{\omega_2^2}{(1+\omega_2)^2}, \quad H_{23}^e = \frac{1}{1+\omega_2}, \quad H_{31}^e = 0, \quad (\omega_2 > 0). \tag{10-b}$$

In eq.(1), ε_{ij}^0 is the external strain corresponding to the external stress σ_{ij}^0, $\tilde{\sigma}_{ij}$ and $\tilde{\varepsilon}_{ij}$ are the interaction stress and strain. The following relationships hold between σ_{ij}^0 and ε_{ij}^0, $\tilde{\sigma}_{ij}$ and $\tilde{\varepsilon}_{ij}$:

$$\sigma_{ij}^0 = C_{ijkl}\varepsilon_{kl}^0, \quad \tilde{\sigma}_{ij} = C_{ijkl}\tilde{\varepsilon}_{kl}. \tag{11}$$

Moreover, $\tilde{\sigma}_{ij}$ is expressed by Mori and Tanaka's theory as

$$\tilde{\sigma}_{ij} = -f\sigma_{ij}^{\infty} = -fC_{ijkl}(S_{klmn}\varepsilon_{mn}^{*} - \varepsilon_{kl}^{*}). \tag{12}$$

where f is the volume fraction of the SMP reinforcement. The equivalent equations for the deviatoric component and the hydrostatic one of the stress and the strain can be written from eq.(1), that is,

$$\mu^{f}\left\{\varepsilon_{ij}^{0\prime} + \tilde{\varepsilon}_{ij}^{\prime} + \left(S_{ijkl} - \frac{1}{3}S_{iikl}\right)\varepsilon_{kl}^{*}\right\} = \mu\left\{\varepsilon_{ij}^{0\prime} + \tilde{\varepsilon}_{ij}^{\prime} + \left(S_{ijkl} - \frac{1}{3}S_{iikl}\right)\varepsilon_{kl}^{*} - \varepsilon_{kl}^{*\prime}\right\}, \tag{13-a}$$

$$K^{f}(\varepsilon_{ii}^{0} + \tilde{\varepsilon}_{ii} + S_{iikl}\varepsilon_{kl}^{*}) = K(\varepsilon_{ii}^{0} + \tilde{\varepsilon}_{ii} + S_{iikl}\varepsilon_{kl}^{*} - \varepsilon_{ii}^{*}). \tag{13-b}$$

where K^{f}, μ^{f} are the bulk modulus and the shear modulus of the SMP reinforcement, respectively, and K, μ are those of the matrix. $\varepsilon_{ij}^{0\prime}$ et al. are deviatoric strains. When the SMP reinforcement is in either the glass state or the transition one, the equivalent eigenstrain ε_{ij}^{*} of the SMP reinforcement is obtained from eq. (13). However, when the SMP reinforcement is in the rubber state, the value of the Poisson's ratio ν^{f} of the SMP reinforcement is 0.5. Therefore, the value of K^{f} is infinity. Then we can't use eq. (13-b) to obtain the unknown ε_{ij}^{*f}. In this case, the following condition that the value of the hydrostatic component ε_{v}^{f} of the elastic strain of the SMP reinforcement is zero[10] is used instead of eq. (13-b),

$$\varepsilon_{v}^{f} = \varepsilon_{ii}^{0} + \tilde{\varepsilon}_{ii} + S_{iikl}\varepsilon_{kl}^{*} = \varepsilon_{ii}^{0} + (1-f)(S_{iikl}\varepsilon_{kl}^{*} - \varepsilon_{ii}^{*}) + \varepsilon_{ii}^{*} = 0. \tag{14}$$

By substituting eqs.(2) and (12) into eqs.(13-b) and (14), we can obtain the following equation,

$$\varepsilon_{ii}^{0} + (1-f)\frac{1-2\nu}{1-\nu}\left\{(H_{1}^{e}-1)\varepsilon_{11}^{*} + (H_{2}^{e}-1)\varepsilon_{22}^{*} + (H_{3}^{e}-1)\varepsilon_{33}^{*}\right\} + L_{K}\varepsilon_{ii}^{*} = 0, \tag{15}$$

where L_{K} is given by

$$L_{K} = \frac{\mu^{f}(1+\nu^{f})(1-2\nu)}{\mu^{f}(1+\nu^{f})(1-2\nu) - \mu(1+\nu)(1-2\nu^{f})}. \tag{16}$$

Eq.(15) is hold regardless of the value of ν^{f}.

In the same way, by substituting eqs.(2) and (12) into eq.(13-a), we can obtain three simultaneous equations with respect to the unknown ε_{ij}^{*}. By applying the relation of eq.(15) to these equations, one of three simultaneous equations is written as,

$$\begin{aligned}
&\left\{\left(\frac{1+\nu}{3}L_{I} - 2L_{II} - 3H_{I}^{e} + 2\right) + 3(H_{2}^{e} - H_{23}^{e}) + (1 - 3H_{1}^{e})\right\}\varepsilon_{11}^{*} \\
&+\left\{\left(\frac{1+\nu}{3}L_{I} + L_{II} - 1\right) + 3(H_{3}^{e} - H_{31}^{e}) + (1-2\nu)(1-3H_{3}^{e})\right\}\varepsilon_{22}^{*} \\
&+\left\{\left(\frac{1+\nu}{3}L_{I} + L_{II} - 1\right) + 3(H_{1}^{e} - H_{12}^{e}) + (1-2\nu)(1-3H_{2}^{e})\right\}\varepsilon_{33}^{*} \\
&= \frac{6(1-\nu)}{1-f}\left(\varepsilon_{11}^{0\prime} - \frac{1}{6}\varepsilon_{ii}^{0}\right),
\end{aligned} \tag{17}$$

where L_I, L_{II} and H_I^e are expressed as

$$L_I = \frac{1}{1+\nu}\left\{\frac{3(1-\nu)}{1-f}L_K - 2(1-2\nu)\right\}, \tag{18-a}$$

$$L_{II} = \frac{2(1-2\nu)}{1-f}\frac{\mu^f}{\mu^f-\mu} - \frac{1}{3}(1-2\nu), \tag{18-b}$$

$$H_I^e = (H_1^e - H_{12}^e) + (H_2^e - H_{23}^e) + (H_3^e - H_{31}^e). \tag{18-c}$$

Coefficients with the subscript of Roman numeral such as L_I and H_I^e are invariants. Other simultaneous equations can be obtained from eq.(17) by the cyclic permutation of subscripts in coefficients and strains except for invariants.

If we solve eq.(17) with respect to the eigenstrain ε_{ij}^*, then,

$$\begin{aligned}\varepsilon_{11}^* = -\frac{1-\nu}{(1-f)(1+\nu)D_0}\Bigg[\Bigg[&(L_{II}+H_I^e-1)^2 - \left\{\frac{3}{2}H_{II}^e + \frac{2}{27}(1-2\nu)^2 H_{III}^e + \frac{2}{3}(1-2\nu)H_{IV}^e\right\}\Bigg]\varepsilon_{ii}^0,\\ &-\frac{2}{3}(1+\nu)\left\{\frac{2}{9}(1-2\nu)H_{III}^e + H_{IV}^e - F_1\right\}\varepsilon_{ii}^0\\ &+2(1+\nu)\left\{L_I(L_{II}+H_I^e-1) - \frac{1}{3}(1-2\nu)H_{III}^e + G_1\right\}\varepsilon_{11}^{0'}\\ &+\frac{2}{3}\Bigg[\left\{(1-2\nu)F_1 - (1+\nu)G_1\right\}\varepsilon_{11}^{0'}\\ &\quad+\left\{(1-2\nu)F_2 - (1+\nu)G_2\right\}\varepsilon_{22}^{0'}\\ &\quad+\left\{(1-2\nu)F_3 - (1+\nu)G_3\right\}\varepsilon_{33}^{0'}\Bigg]\Bigg],\end{aligned} \tag{19}$$

where D_0, F_1, G_1, and R_1 are given by

$$\begin{aligned}D_0 = L_I\Bigg[&(L_{II}+H_I^e-1)^2 - \left\{\frac{3}{2}H_{II}^e + \frac{2}{27}(1-2\nu)^2 H_{III}^e + \frac{2}{3}(1-2\nu)^2 H_{IV}^e\right\}\Bigg]\\ &-\frac{2}{9}(1-2\nu)\left\{(L_{II}+H_I^e-1)H_{III}^e + \frac{2}{3}(1-2\nu)H_V^e + 3H_{VI}^e - H_I^e H_{III}^e\right\}\end{aligned}, \tag{20-a}$$

$$F_1 = (1-3H_1^e)\left\{(L_{II}+H_I^e-1) + 3R_1\right\} \tag{20-b}$$

$$G_1 = \frac{2}{3}(1-2\nu)(1-3H_1^e) + 3L_I R_1, \tag{20-c}$$

$$R_1 = \frac{2}{9}(1-2\nu)(1-3H_1^e) + (H_2^e - H_{23}^e) - \frac{1}{3}H_I^e. \tag{20-d}$$

Other components of F_i, G_i, and R_i can be obtained by the cyclic permutation. In eqs.(19) and (20), $H_{II}^e \sim H_{VI}^e$ are given by

$$H_{II}^e = \left\{(H_1^e - H_{12}^e)^2 + (H_2^e - H_{23}^e)^2 + (H_3^e - H_{31}^e)^2\right\} - \frac{1}{3}(H_I^e)^2, \tag{21-a}$$

$$H_{III}^e = (1-3H_1^e)^2 + (1-3H_2^e)^2 + (1-3H_3^e)^2, \tag{21-b}$$

$$H_{IV}^e=(1-3H_1^e)(H_2^e-H_{23}^e)+(1-3H_2^e)(H_3^e-H_{31}^e)+(1-3H_3^e)(H_1^e-H_{12}^e), \quad (21\text{-c})$$

$$H_V^e=(1-3H_1^e)^3+(1-3H_2^e)^3+(1-3H_3^e)^3, \quad (21\text{-d})$$

$$H_{VI}^e=(1-3H_1^e)^2(H_2^e-H_{23}^e)+(1-3H_2^e)^2(H_3^e-H_{31}^e)+(1-3H_3^e)^2(H_1^e-H_{12}^e). \quad (21\text{-e})$$

A remarkable point of the expression of ε_{11}^* in eq.(19) is that we can obtain easily ε_{ij}^* for two cases, (1) the matrix is an incompressible material and (2) the shape of the SMP reinforcement is a sphere. For the case (1), the value of the Poisson's ratio ν of the matrix is 0.5. Substituting this value into eq.(19), we can derived immediately following explession of ε_{11}^*.

$$\varepsilon_{11}^*=-\frac{2(1-\nu)}{(1-f)\left\{(L_{II}^e+H_I^e-1)^2-\frac{3}{2}H_{II}^e\right\}}\left[\left\{(L_{II}+H_I^e-1)+3(H_2^e-H_{23}^e)-H_I^e\right\}\varepsilon_{11}^{0\prime}\right. \\ \left.-(H_2-H_{23}^e)\varepsilon_{11}^{0\prime}-(H_3-H_{31}^e)\varepsilon_{22}^{0\prime}-(H_1-H_{12}^e)\varepsilon_{33}^{0\prime}\right] \quad (22)$$

For the case (2), by using the relationship in eq.(5) and substituting values of H_i^e and H_{ij}^e in eq.(7) into eq.(19), we can obtain the following explession,

$$\varepsilon_{11}^*=-\frac{1-\nu}{(1-f)(1+\nu)L_I}\left\{\varepsilon_{ii}^*+\frac{2(1+\nu)L_I}{L_{II}-\frac{3}{5}}\varepsilon_{ii}^{0\prime}\right\}. \quad (23)$$

In eq. (23), we should note that the coefficient of $\varepsilon_{11}^{0\prime}$ is expressed only by invariants. Therefore, if the values of external stresses σ_{11}^0, σ_{22}^0, and σ_{33}^0 are same, the values of ε_{11}^*, ε_{22}^*, and ε_{33}^* are also same. Because the property of the material containing spherical reinforcements shows isotropy.

2.4 Macroscopic elastic moduli of the model

The macroscopic average strain of the model $\bar{\varepsilon}_{ij}$ is given by

$$\begin{aligned}\bar{\varepsilon}_{ij}&=\frac{1}{V_D}\int_D(\varepsilon_{ij}^o+\tilde{\varepsilon}_{ij}+\varepsilon_{ij})\,dD \\ &=\varepsilon_{ij}^o+\frac{1}{V_D}\left\{\int_{D-\Omega}(\tilde{\varepsilon}_{ij}+\varepsilon_{ij})\,dD+\int_\Omega(\tilde{\varepsilon}_{ij}+\varepsilon_{ij}-\varepsilon_{ij}^*)\,dD+\int_\Omega\varepsilon_{ij}^*\,dD\right\} \\ &=\varepsilon_{ij}^o+\frac{1}{V_D}C_{ijkl}^{-1}\int_D(\tilde{\sigma}_{kl}+\sigma_{kl}^\infty)\,dD+\frac{1}{V_D}\int_\Omega\varepsilon_{ij}^*\,dD,\end{aligned} \quad (24)$$

where V_D is the volume of the whole body of the model, and ε_{ij} is a strain disturbance. The second term of the right side in eq. (24) is reduced as follows:

$$\frac{1}{V_D}C^{-1}_{ijkl}\int_D(\tilde{\sigma}_{kl}+\sigma^{\infty}_{kl})dD$$
$$=\frac{1}{V_D}C^{-1}_{ijkl}\left\{\int_S(\tilde{\sigma}_{km}+\sigma^{\infty}_{km})x_l\,n_m\,dS-\int_D(\tilde{\sigma}_{km,m}+\sigma^{\infty}_{km,m})x_l\,dD\right\}=0, \tag{25}$$

since the equilibrium condition $\tilde{\sigma}_{km,m}=\sigma^{\infty}_{km,m}=0$ (ex. $\sigma_{ij,j}=\partial\sigma_{ij}/\partial x_j$) in the whole body D of the material and the boundary condition $\tilde{\sigma}_{km}n_m=\sigma^{\infty}_{km}n_m=0$ on the surface S of the body hold, where n_m is the exterior unit normal vector on S. Substituting eq. (25) into eq. (24) and noticing that the equivalent eigenstrain ε^*_{ij} is constant in Ω, we can derive the macroscopic average strain $\bar{\varepsilon}_{ij}$ as follows:

$$\bar{\varepsilon}_{ij}=\varepsilon^0_{ij}+f\varepsilon^*_{ij}. \tag{26}$$

By substituting the equivalent eigenstrain ε^*_{ij} in eq. (19) into eq. (26), we can get the expression of $\bar{\varepsilon}_{ij}$.

The relationships between $\bar{\varepsilon}_{ij}$ and the external stress σ^0_{ij} is expressed as follows:

$$\begin{Bmatrix}\bar{\varepsilon}_{11}\\ \bar{\varepsilon}_{22}\\ \bar{\varepsilon}_{33}\end{Bmatrix}=\begin{pmatrix}1/\bar{E}_{11} & -\bar{\nu}_{12}/\bar{E}_{22} & -\bar{\nu}_{13}/\bar{E}_{33}\\ -\bar{\nu}_{21}/\bar{E}_{11} & 1/\bar{E}_{22} & -\bar{\nu}_{23}/\bar{E}_{33}\\ -\bar{\nu}_{31}/\bar{E}_{11} & -\bar{\nu}_{32}/\bar{E}_{22} & 1/\bar{E}_{33}\end{pmatrix}=\begin{Bmatrix}\sigma^0_{11}\\ \sigma^0_{22}\\ \sigma^0_{33}\end{Bmatrix}, \tag{27}$$

where $\bar{E}_{ij}$ and $\bar{\nu}_{ij}$ are the macroscopic elastic modulus and the Poisson's ratio, respectively. From eq. (27), $\bar{E}_{ij}$ are expressed in terms of $\bar{\varepsilon}_{ij}$, that is,

$$\bar{E}_{11}=\frac{\sigma^0_{11}}{\bar{\varepsilon}_{11}|_{\sigma^0_{22}=\sigma^0_{33}=0}},\qquad \bar{E}_{22}=\frac{\sigma^0_{22}}{\bar{\varepsilon}_{22}|_{\sigma^0_{11}=\sigma^0_{33}=0}},\qquad \bar{E}_{33}=\frac{\sigma^0_{33}}{\bar{\varepsilon}_{33}|_{\sigma^0_{11}=\sigma^0_{22}=0}}. \tag{28}$$

From eqs.(11) and (19), ε^*_{ij} is a function of the external stress σ^0_{ij}. Hence, $\bar{\varepsilon}_{ij}$ in eq.(26) is also a function of σ^0_{ij}. By substituting $\bar{\varepsilon}_{ij}$ in eq. (26) into eq. (28), σ^0_{ij} is vanished and $\bar{E}_{ij}$ is a function of the geometrical factor and elastic constants both of the SMP reinforcement and the matrix.

3. Numerical calculations and discussions

3.1 Elastic properties of the SMP reinforcement

In the present analysis, we assume that the SMP reinforcement is one of the polyurethane series and the glass transition temperature T_g of the SMP reinforcement is 50($^\circ C$). Figure 3 shows the changes in the elastic modulus E^f and the Poisson's ratio ν^f of the SMP reinforcement with temperature T[11]. The SMP reinforcement is in the rubber state at $T>T_g+15(^\circ C)$ and it is in the glass state at $T<T_g-15(^\circ C)$. E^r, ν^r shown in Fig.3 are the elastic modulus and the Poisson's ratio of the SMP reinforcement in the rubber state, respectively, and E^g, ν^g are those in the glass state. When the SMP reinforcement is the transition state at $T_g-15(^\circ C)<T<T_g+15(^\circ C)$, E^f and ν^f are given by[6]

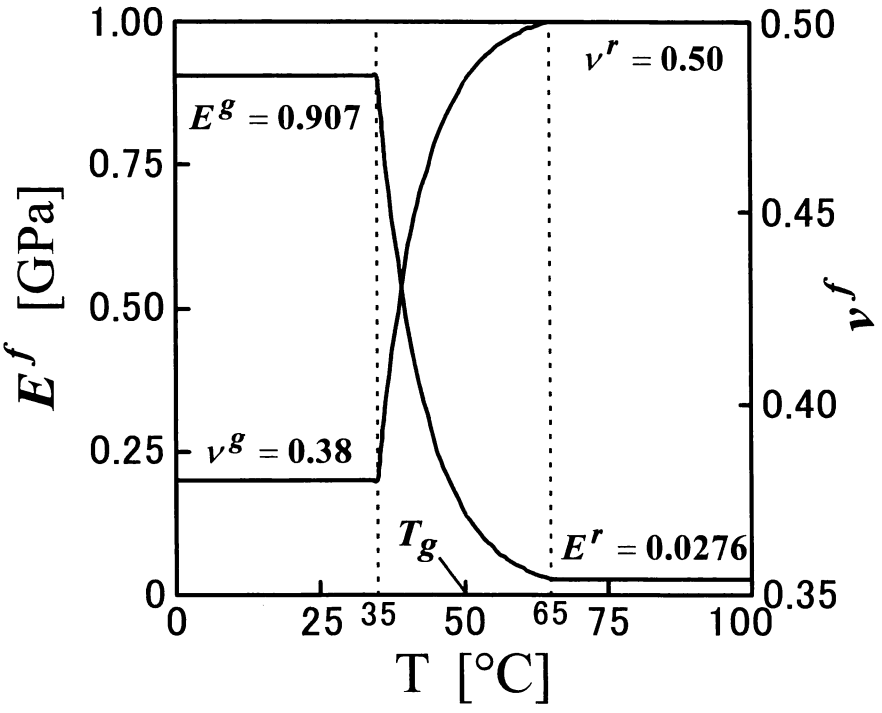

Fig. 3 Changes in the elastic modulus E^f and the Poisson's ratio ν^f of the SMP reinforcement with temperature .

$$E^f = E^g \left(\frac{E^r}{E^g} \right)^{\{(T_g + 15)/30\}\{1 - (T_g - 15)/T\}}, \tag{29-a}$$

$$\nu^f = \frac{\nu^r - \nu^g}{E^r - E^g}(E^f - E^g) + \nu^g. \tag{29-b}$$

3.2 Examination in the value of the elastic modulus of the matrix

In this analysis, the object is to investigate the effect of the shape of the SMP reinforcement on the macroscopic elastic modulus of the material, by utilizing the shape fixity effect of the SMP reinforcement. The shape fixity effect of the SMP reinforcement in the material is occurred by the constraint from the matrix surrounding the SMP reinforcement. Therefore, it is important to examine the value of the elastic modulus of the matrix. Next we consider the effect of the elastic modulus of the matrix on the macroscopic elastic modulus of the material.

Figure 4 shows the change in the macroscopic elastic modulus $\overline{E}_{33}/E$ with the elastic modulus E of the matrix, for various values of the aspect ratio ω_3 of the SMP reinforcement whose shape is spheroid. This shape is shown in Fig. 4. We assume that the shape of the SMP reinforcement is completely fixed at $T < 35(^\circ C)$. As shown in Fig. 4, $\overline{E}_{33}/E$ decreases with increasing E, and becomes $\overline{E}_{33}/E = 1.0$ at point A when $E = E^g$, regardless of the magnitude of ω_3. When the value of E is constant, $\overline{E}_{33}/E$ increases with increasing ω_3. However, when the value of E is over about $0.5(GPa)$, $\overline{E}_{33}/E$ changes little with ω_3. It is desirable that the value of E is higher than E^r from the viewpoint of the shape fixity of the SMP reinforcement, and lower than E^g from the viewpoint that the macroscopic elastic modulus should be at least higher than the elastic modulus of the matrix. These ranges of

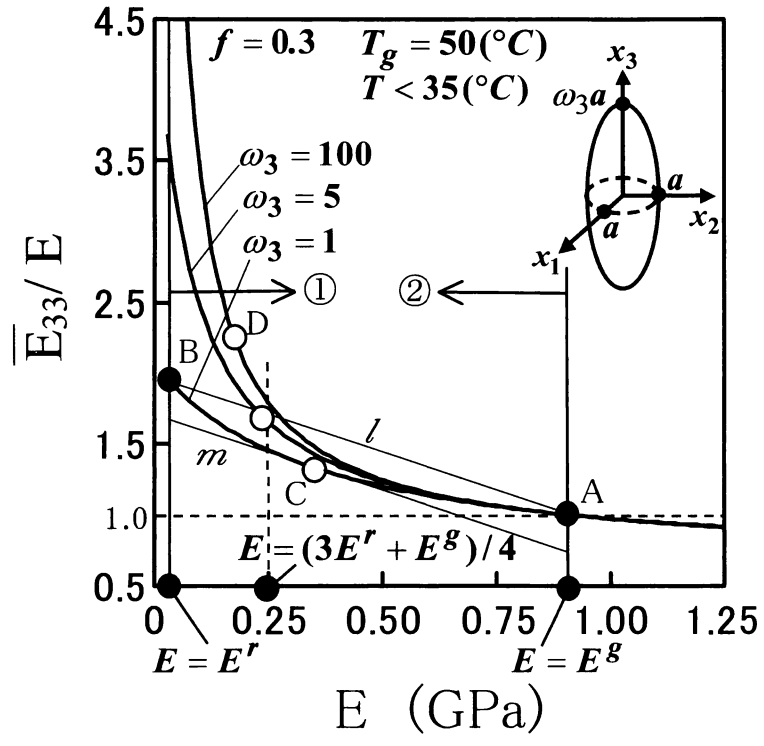

Fig. 4 Changes in the macroscopic elastic modulus $\overline{E}_{33}/E$ with the elastic modulus E of the matrix.

E are denoted by ranges ① and ②, respectively. We consider the suitable value of E by considering these ranges. Our object is to investigate the effect of the aspect ratio of the SMP reinforcement on macroscopic elastic moduli, therefore, it is not preferable to use the value of E over $0.5(GPa)$. Hence, we should decide the value of E, ranging from E^r to $0.5(GPa)$. We see the curve of $\overline{E}_{33}/E$ versus E in the case of $\omega_3 = 1$. Let the point where the curve cuts the line $E = E^r$ be called point B denoted by a solid circle. The line l passes through points A and B. The line m is parallel to the line l and touches the curve at the point C denoted by the open circle. In the same way, other points denoted by open circles for $\omega_3 = 5$ and $\omega_3 = 100$ can be plotted. As E decreases from point D on the curve of $\omega_3 = 100$, the dependence of $\overline{E}_{33}/E$ on ω_3 becomes to be strong. Therefore, the tendency of $\overline{E}_{33}/E$ for the aspect ratio of the SMP reinforcement may be affected greatly by a little change of E. On the other hand, as E increases from point C, the dependence of $\overline{E}_{33}/E$ on ω_3 becomes too small. In taking into consideration with these points, we use the value of E at about the middle point between points C and D, that is, $E = (3E^r + E^g)/4$.

3.3 Changes in macroscopic elastic moduli with temperature

The shape of the SMP reinforcement is assumed to be spheroid, the same as the previous section. Changes in macroscopic elastic moduli $\overline{E}_{22}/E$ and $\overline{E}_{33}/E$ with temperature during the cooling process from a temperature higher than $T_g + 15(°C)$ to that lower than $T_g - 15(°C)$ are illustrated in Figures 5 and 6. Fig. 5 is in the case of $\omega_3 = 100$, and Fig. 6 in the case of $\omega_3 = 0.5$. As shown in Figs. 5 and 6, values of $\overline{E}_{22}/E$ and $\overline{E}_{33}/E$ are constant at $T > 65(°C)$, since the SMP reinforcement is in the rubber state and the elastic modulus E^f of the SMP reinforcement does not change during this range of the temperature as shown in

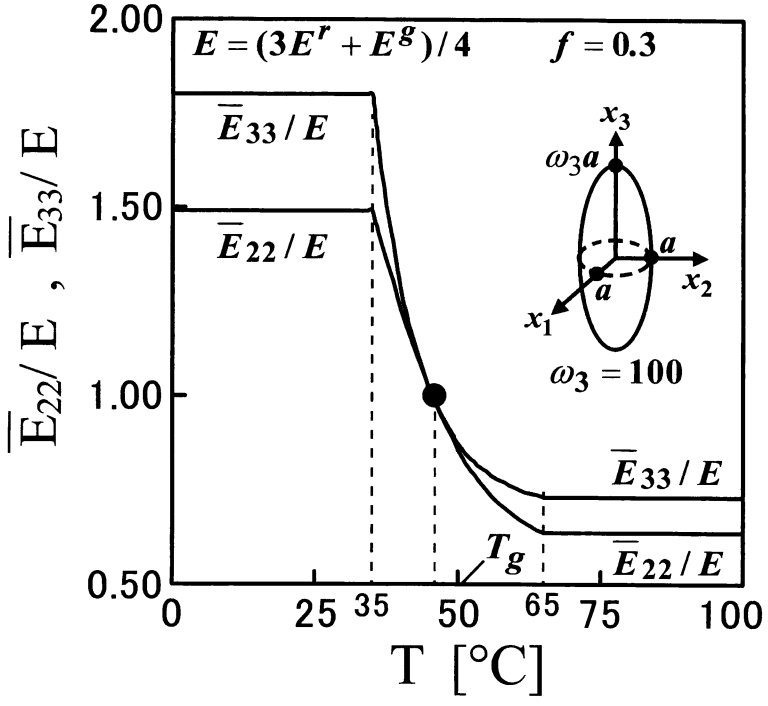

Fig. 5 Changes in macroscopic elastic moduli $\overline{E}_{22}/E$ and $\overline{E}_{33}/E$ with temperature T during the cooling process ($\omega_3 = 100$).

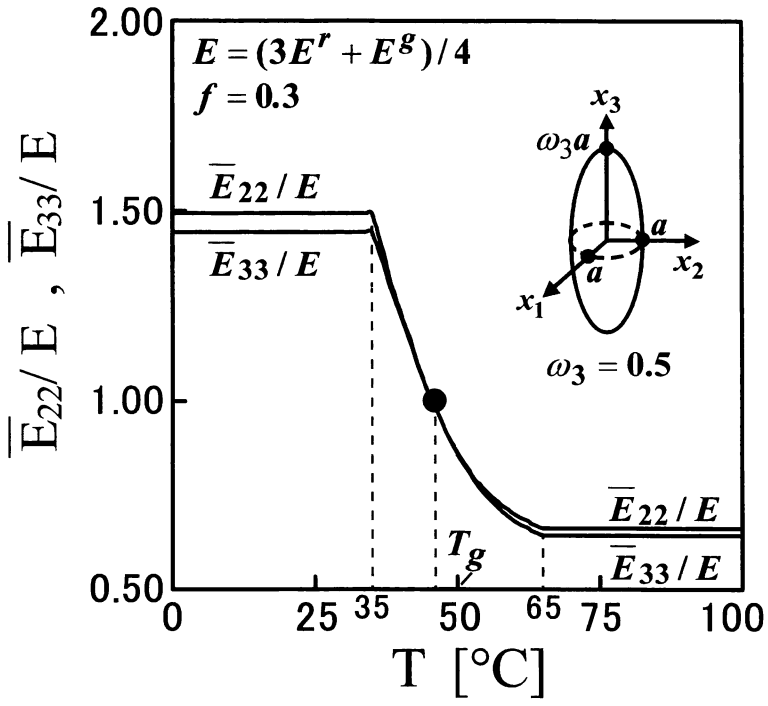

Fig. 6 Changes in macroscopic elastic moduli $\overline{E}_{22}/E$ and $\overline{E}_{33}/E$ with temperature T during the cooling process ($\omega_3 = 0.5$).

Fig. 3. As the temperature decreases from 65(°C), $\overline{E}_{22}/E$ and $\overline{E}_{33}/E$ increase together, since the state of the SMP reinforcement changes from the rubber state to the transition one, and during this change of state, the value of elastic modulus E^f increases. At the solid circle in Figs. 5 and 6, values of $\overline{E}_{22}/E$ and $\overline{E}_{33}/E$ are the same each other, because the magnitude of the elastic modulus of the SMP reinforcement is equal to that of the matrix. As the temperature decreases from this point, values of $\overline{E}_{22}/E$ and $\overline{E}_{33}/E$ increase again. The shape of the SMP reinforcement is fixed completely at $T<35(°C)$, values of $\overline{E}_{22}/E$ and $\overline{E}_{33}/E$ are constant again. In comparing the result in Fig. 5 with that in Fig. 6, we find that macroscopic elastic moduli $T>65(°C)$ at $T<35(°C)$ and greatly depend on the aspect ratio of the SMP reinforcement. In the next section, we will examine this dependence of macroscopic elastic moduli on the aspect ratio of the SMP reinforcement.

3.4 Changes in macroscopic elastic moduli with aspect ratios of the SMP reinforcement

Figure 7 shows changes in macroscopic elastic moduli $\overline{E}_{22}/E$ and $\overline{E}_{33}/E$ with aspect ratios of the SMP reinforcement, at $T>65(°C)$. Fig. 7(a) is in the case of a spheroidal reinforcement, and Fig. 7(b) in the case of an elliptic cylindrical reinforcement. Aspect ratio of SMP reinforcement in Figs. 7(a) and 7(b) are ω_3 and ω_2, respectively. Changes in $\overline{E}_{33}/E$ and $\overline{E}_{22}/E$ are denoted by a solid line and a dotted line, respectively. In Fig. 7(a), as ω_3 decreases from 10^3 to 1, the shape of the SMP reinforcement changes a nearly rod shape, a prolate spheroid, and a sphere in turn. Moreover, as ω_3 decreases from 1 to 10^{-3}, the shape of the SMP reinforcement becomes from a sphere to a oblate spheroid. In Fig. 7(b), as ω_2 increases, the shape of the SMP reinforcement changes from a rod shape to a plate shape

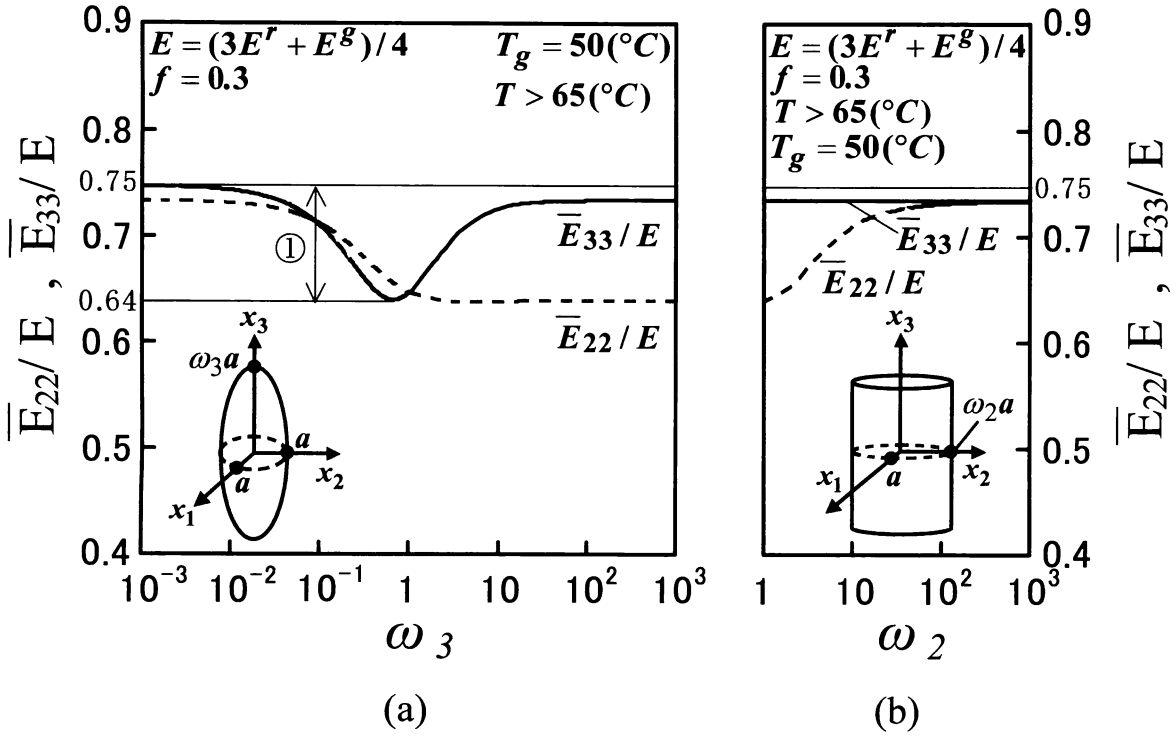

Fig. 7 Change in macroscopic elastic moduli $\overline{E}_{22}/E$ and $\overline{E}_{33}/E$ with aspect ratios ω_2 and ω_3 ($T>65(°C)$). Fig. 7(a) is in the case of the spheroid of the SMP reinforcement, Fig. 7(b) in the case of the elliptic cylinder of the SMP reinforcement.

whose surface is in the x_2-x_3 plane. If the value of ω_3 approaches infinity, the shape of the SMP reinforcement becomes a rod shape. Thus, we note that $\overline{E}_{22}/E$ and $\overline{E}_{33}/E$ at $\omega_3 \to \infty$ in Fig. 7(a) are continually connected with those at $\omega_2 = 1$ in Fig. 7(b).

First, we see Fig. 7(a). As shown in Fig. 7(a), when decreases from 10^3 to about 10^2, $\overline{E}_{33}/E$ is almost constant. As ω_3 decreases from 10^2, $\overline{E}_{33}/E$ also decreases rapidly. At about $\omega_3 = 1.0$, $\overline{E}_{33}/E$ reaches its bottom. On the other hand, $\overline{E}_{22}/E$ is almost constant when ω_3 decreases from 10^3 to about 1. When ω_3 decreases from 1.0, $\overline{E}_{33}/E$ and $\overline{E}_{22}/E$ increase rapidly. Next, we see Fig. 7(b). As shown in Fig .7(b), $\overline{E}_{33}/E$ is almost constant, regardless of ω_2. $\overline{E}_{22}/E$ increases with ω_2, and approaches the constant value of $\overline{E}_{33}/E$.

As shown in Fig. 7, the value of $\overline{E}_{33}/E$ which we can obtain is in the narrow range denoted by ①, that is, $0.64 < \overline{E}_{33}/E < 0.74$. Moreover, both values of $\overline{E}_{22}/E$ and $\overline{E}_{33}/E$ are lower than 1.0 due to the elastic modulus of the SMP reinforcement in rubber state being smaller than that of the matrix. To investigate the effect of the shape of the SMP reinforcement on macroscopic elastic moduli, we need to examine macroscopic elastic moduli under $T < 35(^\circ C)$ at which the shape of the SMP reinforcement is completely fixed.

Figure 8 shows the change only in the macroscopic elastic modulus $\overline{E}_{33}/E$ with aspect ratios of the SMP reinforcement at $T < 35(^\circ C)$. The tendency of $\overline{E}_{33}/E$ for ω_3 in Fig.8 is same as that in Fig.7. From Fig. 8, we find that it is possible to obtain a value of $\overline{E}_{33}/E$ that we want in range ①, $1.44 < \overline{E}_{33}/E < 1.80$, by changing the aspect ratio of the SMP reinforcement. The wide of this range as shown Fig. 8 is about three times as big as that as shown Fig. 7.

Now we consider the shape of SMP reinforcement to obtain a value of $\overline{E}_{33}/E$ that we want. As shown in Fig. 8, at point B, denoted by a solid circle, $\omega_3 = 9.00$ and $\overline{E}_{33}/E = 1.73$.

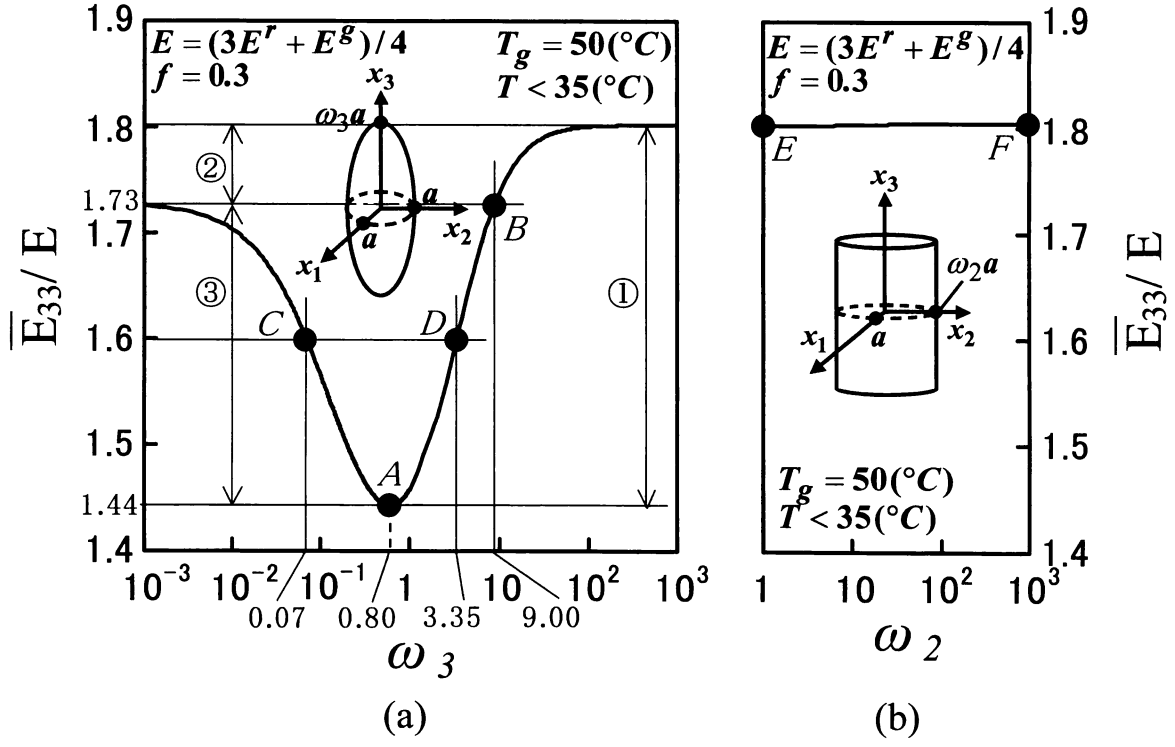

Fig. 8 Change in the macroscopic elastic modulus $\overline{E}_{33}/E$ with aspect ratios ω_2 and ω_3 ($T < 35(^\circ C)$). Fig. 8(a) is in the case of the spheroid of the SMP reinforcement, Fig. 8(b) in the case of the elliptic cylinder of the SMP reinforcement.

The behavior of $\overline{E}_{33}/E$ changes at point B. Therefore, we divide range ① of $\overline{E}_{33}/E$ into two ranges ② and ③. If the value of $\overline{E}_{33}/E$ exists in range ②, there is only one point where the aspect ratio corresponds to the value of $\overline{E}_{33}/E$. But in range ③, for example, when the value that we want to obtain for $\overline{E}_{33}/E$ is 1.6, there are two points, C and D, corresponding to this value of $\overline{E}_{33}/E$, and values of aspect ratios at points C and D are 0.77 and 3.35, respectively. Thus, in range ③, we find that there are two types of the aspect ratio of the SMP reinforcement that values of the macroscopic elastic modulus are same each other.

Figure 9 shows the change in $\overline{E}_{22}/E$ with aspect ratios of the SMP reinforcement, at $T<35(^{\circ}C)$. As shown in Fig.9, points on the curve of $\overline{E}_{22}/E$ corresponding to points C, D, E and F on the curve of $\overline{E}_{33}/E$ in Fig. 8 are indicated by solid circles. First, we see Fig. 9(a). As shown in Fig. 9(a), we find that the values of $\overline{E}_{22}/E$ on points C and D are different from each other. The values $\overline{E}_{22}/E$ on the points C and D are 1.69 and 1.46, respectively. Thus, ratios $\overline{E}_{22}/\overline{E}_{33}$ on the points C and D different from each other. From this result, when a value of $\overline{E}_{33}/E$ exists in range ③ in Fig. 8(a), we can choose alternatively the ratio of $\overline{E}_{22}/\overline{E}_{33}$, that is, the degree of anisotropy of the composite material, by which aspect ratio is given to the SMP reinforcement. However, when the desirable value of $\overline{E}_{33}/E$ exists in range ② in Fig. 8(a), we cannot choose the degree of anisotropy. Next, we see Fig. 9(b). As shown in Fig. 9(b), $\overline{E}_{22}/E$ increases with increasing ω_2, and $\overline{E}_{22}/E$ can have values in a wide range ④, $1.49<\overline{E}_{22}/E<1.80$. That is, regardless of the value of $\overline{E}_{33}/E$ being constant as shown in Fig. 8(b), we can change the value of $\overline{E}_{22}/E$ by the aspect ratio ω_2. Therefore, we can still continually choose the degree of anisotropy of the composite material by changing

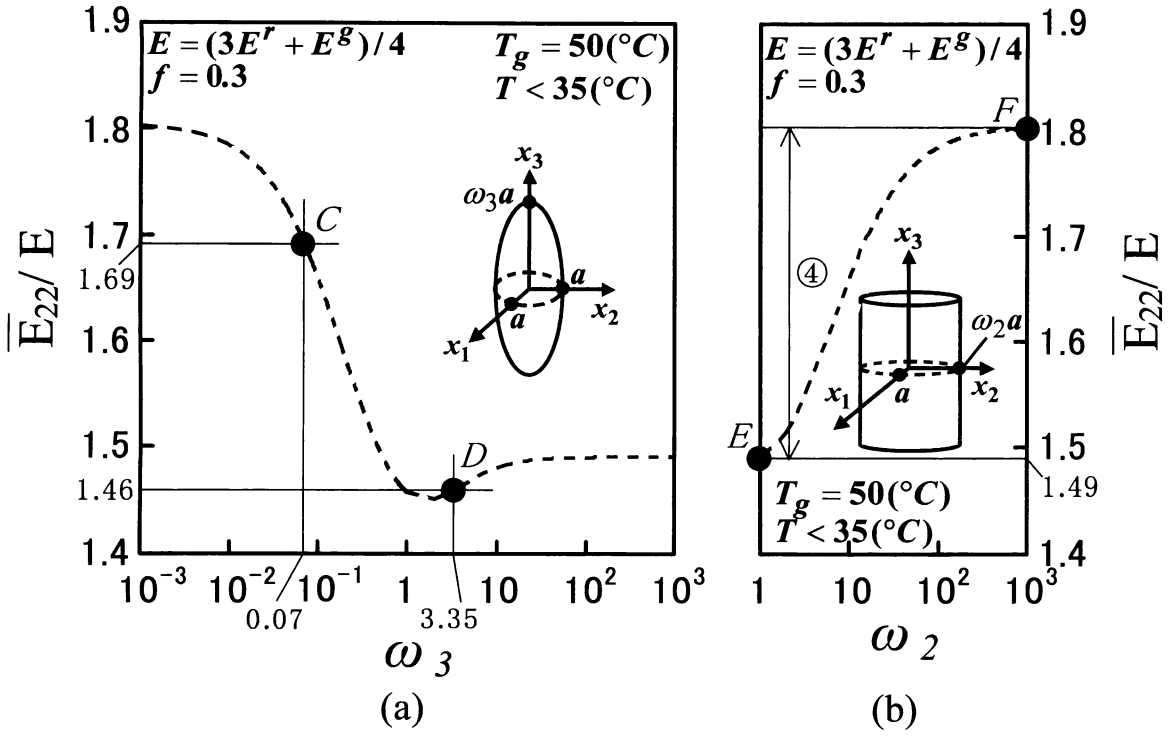

Fig. 9 Change in the macroscopic elastic modulus $\overline{E}_{22}/E$ with aspect ratios ω_2 and ω_3 ($T<35(^{\circ}C)$). Fig. 8(a) is in the case of the spheroid of the SMP reinforcement, Fig. 8(b) in the case of the elliptic cylinder of the SMP reinforcement.

the value of the aspect ratio ω_2.

4. Conclusion

Micromechanical analysis for an intelligent material containing SMP reinforcements is performed by considering the shape fixity effect of the SMP reinforcement. The shape of the SMP reinforcement is modeled as an ellipsoidal one and macroscopic elastic moduli of the material can be formulated as a function of geometrical factors that are related with only aspect ratios of the SMP reinforcement. By using this result, we calculate numerically changes in macroscopic elastic moduli with temperature and effects of aspect ratios of the SMP reinforcement on macroscopic elastic moduli. As a result, we have reached following conclusions.

(1) In the case of a spheroidal SMP reinforcement, changes in macroscopic elastic moduli of the model with temperature during the cooling process to fix the shape of the SMP reinforcement could be obtained. And values of macroscopic elastic moduli at $T > T_g + 15(^\circ C)$ and $T < T_g - 15(^\circ C)$ greatly depend on the aspect ratio of the SMP reinforcement.

(2) Then, we calculate changes in macroscopic elastic moduli with aspect ratios of the SMP reinforcement at $T > T_g + 15(^\circ C)$ and $T < T_g - 15(^\circ C)$. In the result, at $T < T_g - 15(^\circ C)$ it is possible to obtain a desirable value of the macroscopic elastic modulus in a certain range by changing the aspect ratio of the SMP reinforcement. The wide of this range is about three times as big as that at $T > T_g + 15(^\circ C)$. Especially, in the case of the spheroidal reinforcement, there are two aspect ratios that values of the macroscopic elastic modulus in the rotational axis of the SMP reinforcement are same each other. Moreover, values of the macroscopic elastic modulus in the direction normal to the rotational axis, which is obtained from above two aspect ratios, are different from each other. It means that we can alternatively choose degree of anisotropy on stiffness of the material by which aspect ratio is given to the SMP reinforcement.

(3) On the other hand, in the case of an elliptic cylindrical SMP reinforcement, even though the value of elastic modulus in a longitudinal direction is nearly constant regardless of the aspect ratio, the macroscopic elastic modulus in the direction normal to the longitudinal direction have a wide range of value. That is, we can continually choose degree of anisotropy of the material on the stiffness.

From above-mentioned results, we can suggest that it is possible to change degree of anisotropy of the material on the stiffness by utilizing the shape fixity effect of the SMP reinforcement.

Acknowledgments

The present work was supported by a Grant-in Aid for Scientific Research (No. 15760523) from the Ministry of Education, Culture, Sports, Science and Technology of Japan.

Department of Mechanical and System Engineering,

Faculty of Engineering and Design,
Kyoto Institute of Technology,
Matsugasaki, Sakyo-ku, Kyoto 606-8585 JAPAN

References

1) JSME ed., "Intelligent Composite Material and Intelligent Adapted structures", pp.1-55, Yokendo Ltd. (1996).
2) A.Shimamoto and M.Taya, *Trans. JSME, Ser.A*, **63**, 605, pp.26-31 (1997).
3) H.Ono, S.Araki, and K.Saito, *Theoretical and Applied Mechanics*, **49**, pp.299-309 (2000).
4) S.Araki, H.Ono, S.Yamada, and K.Saito, *Trans. JSME, Ser.A*, **67**, 659, pp.1140-1147 (2001).
5) S.Araki, H.Ono, and K.Saito, *Trans. JSME, Ser.A*, **68**, 666, pp.244-252 (2002).
6) S.Araki, H.Ono, and K.Saito, *Trans. JSME, Ser.A*, **68**, 666, pp.253-257 (2002).
7) H.Tobushi and S.Hayashi, *Science of Machine*, **45**, 11, pp.1136-1141 (1993).
8) T.Mura, "Micromechanics of Defects in Solids, Second revised edition", pp.74-84, Kluwer Academic Publishers (1987).
9) S.Araki, H.Yamashita, and A.Minami, *Trans. JSME, Ser.A*, **71**, 701, (2005), pp.157-164.
10) K.Saito, S.Araki, and T.Nakamura, *Mechanics of Composite Materials*, **32**, pp.317-329 (1996).
11) H.Tobushi, S.Hayashi, E.Yamada, and T.Hashimoto, *Trans. JSME, Ser.A*, **64**, 617, pp.186-192 (1998).